RI 9622

REPORT OF INVESTIGATIONS/1996

Comparative In-Mine Evaluation of Carbon Monoxide and Smoke Detectors

By John C. Edwards and Gene F. Friel

UNITED STATES DEPARTMENT OF THE INTERIOR

UNITED STATES BUREAU OF MINES

Report of Investigations 9622

Comparative In-Mine Evaluation of Carbon Monoxide and Smoke Detectors

By John C. Edwards and Gene F. Friel

UNITED STATES DEPARTMENT OF THE INTERIOR
Bruce Babbitt, Secretary

BUREAU OF MINES
Rhea Lydia Graham, Director

CONTENTS

ILLUSTRATIONS

TABLES

UNIT OF MEASURE ABBREVIATIONS USED IN THIS REPORT

cm	centimeter	m^3/(particle·s)	cubic meter per particle per second
cm/min	centimeter per minute	mA	milliampere
kg	kilogram	mL	milliliter
kg/m^3	kilogram per cubic meter	mV	millivolt
L	liter	pct	percent
m^{-1}	inverse meter	ppm	part per million
m	meter	s	second
m^2	square meter	V	volt
m/s	meter per second	μm	micron
m^3/s	cubic meter per second		

COMPARATIVE IN-MINE EVALUATION OF CARBON MONOXIDE AND SMOKE DETECTORS

By John C. Edwards[1] and Gene F. Friel[2]

ABSTRACT

A series of liquid fuel fire experiments evaluated the comparative responses of five types of commercially available smoke detectors and a diffusion-mode carbon monoxide (CO) detector under normal and reduced airflow conditions based upon the alarm times of the detectors. These experiments were conducted in the Safety Research Coal Mine at the U.S. Bureau of Mines Pittsburgh Research Center. Two of the smoke detectors had manufacturer set alarms. For the other three smoke detectors, an alarm point was defined in terms of their background analog signal and the detector's electrical output noise under ambient conditions. A correlation was developed of the travel time of 5 ppm CO between pairs of CO detectors with the travel time calculated from entry and crosscut volumes and measured airflow. Based upon the relative performance of smoke detectors in this limited study, smoke detectors can be as effective as CO detectors for mine fire detection once identifiable alarm values are defined. Implementation of smoke detectors as part of an atmospheric mine monitoring system will improve mine safety.

[1]Research physicist.
[2]Chemical engineer.
Pittsburgh Research Center, U.S. Bureau of Mines, Pittsburgh, PA.

INTRODUCTION

Currently, the CO detector is the more common detector used for fire detection as part of atmospheric monitoring system in underground mines. In recent years, smoke detectors have been evaluated in several mines (*1*).[3] It also was shown that the performance of smoke detectors can be evaluated in the laboratory with the use of a smoke chamber (*2*) for smoldering and flaming coal combustion. Subsequently, a relative evaluation of six smoke detectors was made with the smoke chamber (*3*). Those studies showed, based upon analysis of the smoke detector's analog response signal, that it is possible to detect the occurrence of smoke from coal combustion when the optical density is less than 0.022 m^{-1}. It was further demonstrated that the optical density of 0.022 m^{-1} corresponded to a measurable CO concentration of 5 ppm above ambient for smoldering and flaming coal combustion. This U.S. Bureau of Mines (USBM) research was undertaken to enhance the safety of mine workers through the utilization of an improved atmospheric mine monitoring system.

In order to make a comparison of the responses of CO and smoke detectors to an in-mine fire, a series of experiments was conducted by the USBM in the Safety Research Coal Mine (SRCM) located at the Pittsburgh Research Center. A previous USBM experimental study (*4*) showed that dead-end crosscuts affect the transport time between CO detectors by providing an entrainment mechanism for dilution of the CO concentration in the entry. The complex geometric characteristics of smoke particulates, such as size distribution and concentration, and physical properties, such as dielectric constant, could result in a variable response time of smoke detectors compared to CO detectors. This is in addition to expected differences in measurable responses based upon whether the detector operates in a diffusion mode or a pump mode. The effect of ventilation flow and entrainment at dead-end crosscuts on the responses of CO and smoke detectors at nearly identical locations will provide a basis for future recommendations for the implementation of improved atmospheric monitoring systems in mines. For this study, a mine combustible, diesel fuel, provided the smoke and CO source. The practical advantage of diesel fuel as a combustion source is its relatively uniform production of smoke and CO. For 2 of the 12 experiments, conveyor belt strips were used to increase CO production. For the other 10 experiments, a small quantity of gasoline was added to the diesel fuel to assure uniform ignition of the diesel fuel. Normal airflow conditions in excess of 1.0 m/s and reduced airflow conditions with air velocities less than 0.4 m/s were considered.

EXPERIMENTAL PROCEDURES

A plan view of the SRCM section used for the experiments is shown in figure 1; the airflow direction is also shown. F Butt was instrumented with CO and smoke detectors for each experiment. The total separation distance from the first to the last sensor in F Butt was 91 m. The source fire was located in the mine portal, approximately 360 m from Station No. 1. Smoke detectors from five different manufacturers and CO detectors from two different manufacturers were used for the experiments. Table 1 lists the primary detectors used for most of the experiments at the stations indicated, the operational type as either ionization or optical for the smoke detectors, and the sampling mode as either diffusion or pump. The maximum measured output signal of smoke detector A for the fire experiments was approximately 2.5 V, with a background of 0.13 V in clear air. The alarm of smoke detector B is 2.5 V on a 1- to 5-V range. Unlike the other smoke detectors, which have an accessible analog output signal, smoke detector C has two discrete output signals. For clear air the signal is 4 mA; for smoke-laden air the signal is 20 mA. Smoke detector D is calibrated to read 0.4 V in clear air and 2.0 V when the smoke obscuration is equivalent to an optical density of 0.046 m^{-1}. The output signal range of smoke detector E is -0.9 to -0.2 mA, which was converted electronically to 0.9 V for clear air to 0.2 V for air saturated with smoke. Smoke detectors A and B operate in the mechanical pump mode, whereas smoke detectors C, D, and E operate in the diffusion mode. A and D are based upon optical detection principles, whereas B, C, and E are based upon ionization principles.

Table 1.—Primary product of combustion detectors used in mine fire experiments

Station	Detectors	
	Carbon monoxide	Smoke (type, sampling mode)
1	CO-1, CO-2	E (I, D)
2	CO-1	A (O, P)
3[1]	CO-1	B (I, P)
4	CO-1	C (I, D)
5	CO-1	D (O, D)
6	CO-1, CO-2	E (I, D)

[1]Also light obscuration meter.
I Ionization.
O Optical.
D Diffusion.
P Pump.

Two different types of CO detectors were used. One type of CO detector, CO-1, operates in a diffusion mode, and the other type, CO-2, operates in a mechanical pump mode. Both CO-1 and CO-2 operate on the principle of electro-oxidation of oxygen, although with different types of chemical cells. Additonal

[3]Italic numbers in parentheses refer to items in the list of references at the end of this report.

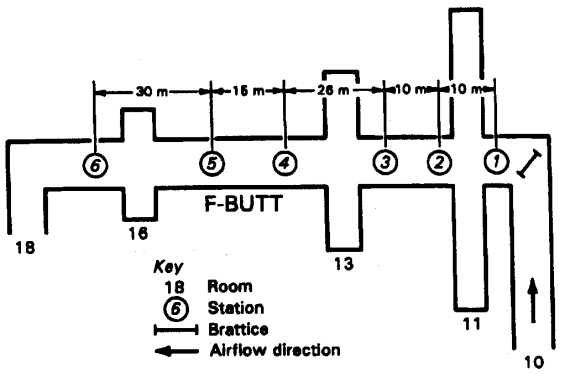

Figure 1.—Plan view of the mine section used for the experiments.

CO detectors of type CO-1 were located in crosscuts (rooms 11, 13, and 16). Also, pairs of the CO-1 CO detector were suspended at Stations 1 through 6.

To measure the optical obscuration in the smoke, an optical obscuration meter was constructed. This consisted of a halogen lamp source and a photovoltaic cell separated by a distance of 1 m. The lamp and photo cell were supported in a rigid frame constructed from 10-cm-diameter plastic pipe with diametrically opposed openings spaced along the length of the pipe to permit smoke-laden air to cross the optical path. The frame was mounted at mid-height such that the optical path was transverse to the airflow along the airway. Complete mixing over the entry cross-section is expected at this location. The entrance port to each detector was about 0.4 m from the roof. For the diffusion CO sensors, the tilt of the diffusion tube was approximately 20° upwind. This orientation provides for optimal sensor operation, as reported earlier (*4*).

The analog signals from each CO and smoke detector, as well as from the light obscuration meter, were converted to digital signals and collected by a computer monitoring system. Data sampling occurred at 2-s intervals.

Air quantity in the mine section was controlled by adjustment of the fan pitch and installation of brattices in the SRCM. To ensure an even distribution of air quantity at the entrance to F Butt, a brattice was positioned oblique to the entrance of F Butt as shown in figure 1.

Smoke detectors were positioned along the centerline of F Butt. Adjacent to each smoke detector was a diffusion-mode CO detector, CO-1. For several of the experiments, a pump-mode CO detector, CO-2, was located at the entrance of F Butt, and at the far downwind position of F Butt.

Prior to ignition of the diesel fuel source for each experiment, a ventilation survey was made of the mine section. The ventilation was generally measured 1.8 m upwind of the sensors in the entry. Since most velocity measurements contained wind and fan fluctuations, 5- and 9-point time-averaged flow measurements were made during the ventilation survey. Smoke-tube measurements of the airflow were made in selected crosscuts.

The CO sensors were calibrated with a zero and span gas. It was occasionally noted during the course of the experiments that, even though a chemical cell for a sensor would hold its calibration, a deterioration in the performance of the cell was associated with a lag in the sensor response. This was indicated by an unusually long decay back to the ambient concentration from the maximum concentration. This was verified by the interchange of two sensors, located adjacent to each other at the same downwind position in the entry, and a repetition of the experiment. If the concentration measurements of the interchanged sensors were reproducible, then a deterioration in the chemical cell of the CO sensor was verified, and the cell was replaced. The normal expected useful lifetime of a chemical cell would decrease through repetitive use in an environment with CO and other product-of-combustion gases associated with fire tests.

Each smoke detector was adjusted according to the manufacturer's specifications. The amplifier circuit on the photocell used in the light obscuration meter was adjusted prior to each experiment so that the output of 1 V corresponded to 100 pct optical transmission through clear air.

After calibration of the sensors and completion of the ventilation survey, the fuel tray was placed in the mine portal. Square tray sizes of 0.46 m side length and 0.76 m side length were used. It was determined that inadequate CO was generated from a diesel fuel fire in a 0.46-m side-length tray. For this reason, conveyor belt strips were mounted on the rim of the tray above the diesel fuel to increase the CO production through their combustion. Although this measure increased the CO, it was not adequate to assure that 5 ppm of CO above background was less than the inflection point on the CO concentration versus time profile at a sensor location. This is important for application of the analysis of previous work (*4*) to transport time between sensors based upon entry and crosscut volume. For this reason, a tray with a 0.76 m side length was used for the remainder of the experiments in which the fire was located in the mine portal. It was found by trial and error that the addition of 500 mL of gasoline to the diesel fuel assured rapid, uniform burning of the diesel fuel.

In order to observe the effect of ventilation on flame tilt, a pole was mounted vertically about 1 m downwind of the fire for several experiments. Visual observations were made of the flame tilt at 15-cm intervals marked on the pole. From the horizontal distance between the pole and the fire, and the vertical position on the pole intersected by a straight line from the extended flame, the angle of tilt of the flame was determined for the experimental conditions of ventilation and fuel surface area.

A summary of the fire experiments conducted in the SRCM is presented in table 2. The experiments are characterized by fuel tray size, fuel loading, average measured airflow quantity in F Butt, and the crosscut accessibility for the airflow in F Butt.

Experiments 1-9 were conducted under normal mine ventilation conditions. Experiments 10-12 were conducted to investigate the responses of smoke and CO detectors under reduced airflow conditions. For experiments 1-9, the air quantity at the entrance to F Butt was 8 to 11 m^3/s. Leakage along the

Table 2.—Experimental conditions

Experiment	Tray size, m	Diesel fuel, L	F Butt air quantity, m^3/s		Crosscuts
			Station 1	Station 6	
1[1]	0.46 by 0.46	2.0	9.8	8.4	Closed.
2[1]	0.46 by 0.46	2.0	9.8	8.1	Closed.
3.....	0.76 by 0.76	4.0	9.1	7.4	Closed.
4.....	0.76 by 0.76	4.0	8.9	7.4	Open.
5.....	0.76 by 0.76	3.5	10.2	7.8	Closed.
6.....	0.76 by 0.76	3.5	9.3	7.9	G Butt side open; E Butt side closed.
7.....	0.76 by 0.76	3.5	9.0	8.3	G Butt side closed; E Butt side open.
8.....	0.76 by 0.76	3.0	8.9	7.2	Open.
9.....	0.76 by 0.76	3.0	9.5	7.3	Closed.
10	0.76 by 0.76	4.0	1.8	3.0	Open.
11	0.76 by 0.76	4.0	3.0	3.0	Open.
12	0.46 by 0.46	2.0	2.5	2.1	Open.

[1]Three strips of conveyor belt 0.53 m by 5.1 cm by 1.1 cm were mounted over top of tray.

airway through the crosscuts reduced this to 6 to 9 m^3/s at the exit of F Butt. For experiment 10, a brattice was positioned as an airflow regulator at entrance room 10 to reduce the airflow in F Butt. A reduction in air quantity was achieved in F Butt. However, a positive differential pressure was created from a parallel entry into F Butt. This resulted in air leakage from the parallel entry into F Butt through the brattices separating the connecting rooms of the airways. This resulted in dilution of the CO along F Butt. To correct this condition, a brattice was positioned as a regulator at the junction of F Butt and room 18 for experiments 11-12. This increased the pressure of F Butt relative to the parallel airway, and prevented dilution of the CO in F Butt due to air leakage from the parallel entry.

The linear airflow in F Butt varied from 0.8 to 1.2 m/s for experiments 1-9, whereas for experiments 10-12, the linear airflow was less than 0.4 m/s. For experiment 12, the fire source was moved from the portal to Room 10, about 45 m from the junction of room 10 and F Butt, to increase the smoke concentration in F Butt.

RESULTS

Experiments 3-12 resulted in nearly uniform ignition and combustion of diesel fuel because of the addition of a small quantity of gasoline to the diesel fuel. Experiments 3-11 were conducted with a 0.76-m side-length tray, and experiment 12 was conducted with a 0.46-m side-length tray. For experiments 3-11, the average linear burning rate of the fuel was between 0.07 and 0.17 cm/min, with an average rate of 0.12 cm/min. The burning rate for experiment 12 was 0.19 cm/min. These burning rates are lower than the values of 0.2 cm/min and 0.3 cm/min for 0.46- and 0.76-m-diameter pans, respectively, as reported in previous work in zero airflow conditions (*5*). This could be an effect of the ventilation. Experiments 3-11 differed from experiment 12 not only in tray size (side length of 0.76 m for experiments 3-11 and 0.46 m for experiment 12), but in the ventilation flow at the fire location. The fire was located in the mine portal for experiments 3-11, where the average ventilation linear speed was approximately 2 m/s. For experiment 12, the fire source was located in a reduced airspeed (about 0.4 m/s) section of the mine.

A visual observation of flame tilt was made relative to a vertical pole 1.07 m downwind from the fire with 15-cm markers on the pole. Thomas (*6*) reported correlations of the convective wind-induced tilt of a flame based upon data from wood crib fires. A study by the American Gas Association (AGA) (*7*) also reported a correlation of flame tilt with wind velocity. For a diesel-fuel experiment with a 0.46-m side-length tray, and a wind speed of 1.86 m/s, flame tilt of 47° to 59° from the normal line to the horizontal fuel surface was observed. Thomas' model predicts a tilt angle of 76°, whereas the AGA model predicts a tilt of 70°. These predictions are significant overestimates of the measured tilt. The comparison of measured flame tilt with model predictions is somewhat closer for the AGA model with a relative error between 16 and 33 pct. Flame tilt dependence upon ventilation is important for determination of flame propagation over a fuel surface.

Table 3 identifies the minimum optical transmission over a 1-m path length that occurred for each experiment. Experiments 1 and 2 were conducted with a sufficiently small fuel tray size such that the optical transmission did not decrease below 90 pct for the ventilation used. This optical transmission corresponds to an optical density of 0.046 m^{-1}. Experiments 3-8 were conducted with a larger tray size than experiments 1 and 2, and had significantly lower values for minimum optical transmission. Optical transmission data were not available for experiment 9. Experiments 10 and 11 had high optical transmissions because the airflow primarily bypassed F Butt, where the optical obscuration meter was located, and passed through a parallel entry. Experiment 12 had a relatively low optical transmission because the fire was located in reduced airflow in Room 10 connected to F Butt, even though the tray size for experiment 12 was the same as for experiments 1 and 2.

Table 3.—Minimum optical transmission, optical density at alarm time of smoke detector B and comparison of alarm times of smoke detectors B and C with CO detector

Experiment	Minimum optical transmission, pct	D, m^{-1}	$\Delta\tau$(CO, B), s	$\Delta\tau$(CO, C), s
1	91	0	132	NA
2	92	0	147	NA
3	53	0.033	52	21
4	60	0.044	36	18
5	57	0.026	42	18
6	69	0.025	53	21
7	59	0.021	53	8
8	70	0.017	40	15
9	NA	NA	NA	18
10	89	0.0070	80	NA
11	95	0.0035	NA	NA
12	57	0.054	60	33

NA Not available.

At Station 2, smoke detector A was positioned next to a type CO-1 CO detector. Figure 2 shows the responses of smoke detector A and CO detector CO-1 for experiment 4. An alarm was defined for smoke detector A for each experiment as the average background signal plus 10 standard deviations of the detector's noise under ambient conditions. For normal airflow experiments 3-8, smoke detector A's alarm occurred an average of 17 s after the alarm of the adjacent CO detector CO-1. Data were not available for smoke detector A for experiment 9. For experiments 1, 2, 10, and 11, characterized by dilute CO concentrations and higher minimum optical transmissions, smoke detector A's alarm occurred prior to the CO alarm. The alarm times of smoke detector A and CO alarm CO-1 were nearly simultaneous for experiment 12. For experiments 1, 2, 10, and 11, smoke detector A's output voltage had increased by more than 300 mV when the adjacent CO sensor alarmed. The fires for these particular experiments were characterized by minimum optical transmissions over a 1-m distance that were greater than 89 pct. For fire experiments 3-8 and 12 with the more intense fires and associated minimum optical transmissions of less than 70 pct over 1 m, smoke detector A's output voltage increased by 30 mV when the CO sensor reached alarm stage. Although the minimum optical density is used to refer to fire intensity, this is not a true measure of fire intensity since air dilution controls the smoke intensity as measured by the optical transmission. The earlier alarm time of smoke detector A for less intense fires, compared with when the CO-1 detector reached alarm, implies that, at least for the fire size and growth rate developed, smoke detector A could be more sensitive for fire detection of low intensity fires than the CO detector, dependent on the CO alarm level.

At Station 3, smoke detector B was positioned adjacent to the CO-1 CO detector. Figure 3 shows the comparative responses of smoke detector B and CO detector CO-1 for experiment 4. The initial responses of both the CO-1 detector and smoke detector B are almost coincidental even though the CO detector is a diffusion mode, and the smoke detector operates in the pump mode. Table 3 provides an evaluation of the optical density at which smoke detector B alarmed. The average optical density at smoke detector B's alarm was 0.021 m^{-1}, and the standard deviation was 0.018 m^{-1}. The CO concentration at Station 3 was less than 1 ppm above background when smoke detector B alarmed. For experiments 3-8 and 10-12, which had only diesel fuel as the combustion source, the optical density at which the smoke detector B alarmed ranged from 0.0035 to 0.054 m^{-1}, with an average value of 0.026 m^{-1} and a standard deviation of 0.016 m^{-1}. For the normal airflow experiments 3-8, the average optical density at which smoke detector B alarmed was 0.028 m^{-1}, while for the reduced airflow experiments 10-12, the average optical density at alarm was 0.022 m^{-1}. For experiments 3-8, 10, and 12, the average optical density when the diffusion-mode CO-1 detector reached 5 ppm above ambient was 0.085 m^{-1} with a standard deviation of 0.046 m^{-1}. A comparison was made of the alarm times of CO detector CO-1 and smoke detector B. In each case, smoke detector B's alarm time occurred prior to that of the CO detector. This is listed in table 3 as $\Delta\tau$(CO, B), where $\Delta\tau$(X, Y) is defined as the differential time by which detector X's alarm time follows detector Y's alarm time. In addition to having an earlier alarm time than the CO detector, smoke detector B gave a significantly earlier alarm time for those experiments with less intense fire sources, as characterized by the minimum optical transmissions listed in table 3. In particular, experiments 1, 2, and 10 with minimum optical transmissions over a 1-m distance greater than 89 pct, had values of $\Delta\tau$ (CO, B) greater than 80 s. For experiment 9, smoke detector B was not operational and for experiment 11, the CO detector at Station 3 was not reliable.

Figure 4 shows the response of the light obscuration meter for experiment 4. A comparison of figures 3 and 4 shows that the CO maximum concentration is approximately 50 s after the minimum optical transmission. This is a characteristic indicative of the response time of the chemical cell in the CO detector.

A significant difference between average optical densities of the CO alarm was determined based upon airflow. For normal airflow experiments 3-8, the average optical density at which the CO-1 detector was 5 ppm above ambient, was 0.11 m^{-1}, whereas for reduced airflow experiments 10 and 12, the average optical density at alarm was 0.017 m^{-1}. When the measured optical density was 0.022 m^{-1}, the average measurable CO concentration was less than 1 ppm above background for experiments 3-8. For experiments 10-12, the CO concentration was less than 4 ppm

above background at an optical density of 0.022 m^{-1}. However, as pointed out above, the diffusion-mode response time of the CO sensor does not permit a simultaneous measurement of CO concentration and optical density.

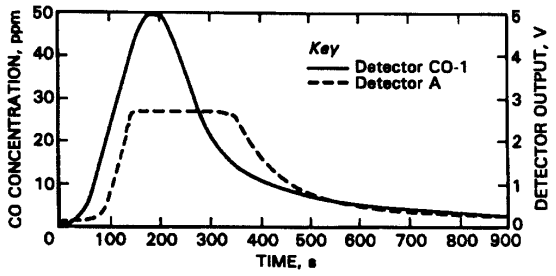

Figure 2.—Comparison of measured CO concentration and response of smoke detector A at Station 2 for experiment 4.

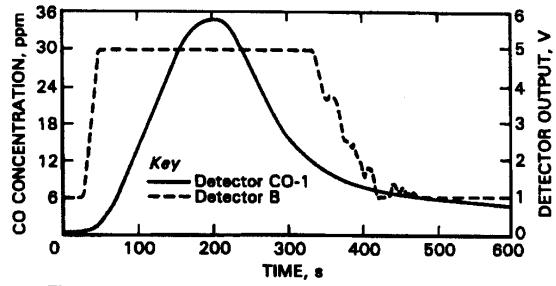

Figure 3.—Comparison of measured CO concentration and response of smoke detector B at Station 3 for experiment 4.

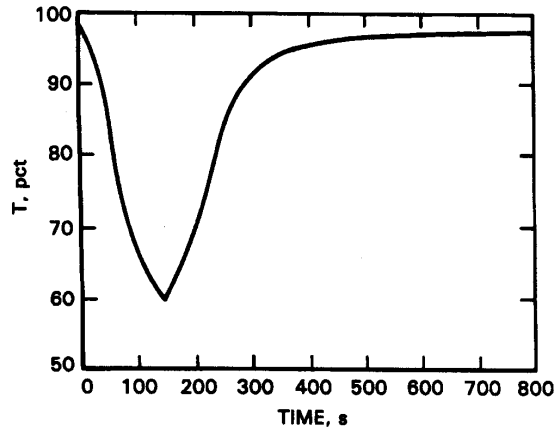

Figure 4.—Response of light obsuration meter at Station 3 for experiment 4.

Smoke detector C was located at Station 4 adjacent to a CO-1 CO detector. The responses of the CO and smoke detectors are shown in figure 5 for experiment 4. Table 3 shows a comparison of the alarm time for CO-1 detector with smoke detector C through an evaluation of $\Delta\tau$(CO, C). For experiments 1, 2, 10, and 11, smoke detector C did not alarm. In each of these experiments, the minimum optical transmission over a 1-m distance was greater than 89 pct (optical density less than 0.051 m^{-1}). For those experiments for which smoke detector C alarmed, it alarmed prior to the CO alarm and the optical density was greater than 0.15 m^{-1}. When a comparison is made between the alarm time of smoke detector C relative to the alarm time of its adjacent CO detector, and the alarm time of CO smoke detector B relative to the alarm time of its adjacent CO detector, quite dissimilar results are observed. For experiments 1, 2, and 10 with higher minimum optical transmission, detector B responds much earlier than the diffusion-mode CO detector. However, for these same experiments, smoke detector C does not alarm. This could be a consequence of the pump-mode characteristic of smoke detector B in comparison with the diffusion-mode characteristic of smoke detector C.

For experiments with nearly the same minimum optical transmissions, the effect of airflow on $\Delta\tau$(CO, B) and $\Delta\tau$(CO, C) was assessed. Table 3 shows that $\Delta\tau$(CO, B) and $\Delta\tau$(CO, C) are somewhat, but not significantly, higher for reduced airflow experiment 12 in comparison with the normal airflow experiments 3-8.

At Station 5, a type CO-1 CO detector and smoke detector D were positioned near the roof. Figure 6 shows the responses of the CO-1 detector and smoke detector D for experiment 4. Both detectors show a nearly coincidental response time to the products of combustion. The maximum response of smoke detector D occurred prior to the maximum response of the CO-1 detector. Since both smoke detector D and the CO-1 detector are diffusion-mode detectors, the difference in response time at maximum signal is primarily due to the instantaneous response of the optical smoke detector compared to the response time characteristic of the chemical cell in the CO detector. An alarm was defined for smoke detector D for each experiment in the same manner as the definition of the alarm for detector A, the average background signal plus 10 standard deviations of the detector's noise under ambient conditions. Detector D alarmed for each experiment based upon this criterion. For normal airflow experiments 3-9, smoke detector D alarmed an average of 63 s prior to the adjacent CO-1 detector. The CO detector did not alarm for experiments 1 and 11; and for experiments 2, 10, and 12, the CO alarm occurred 175, 156, and 93 s, respectively, after the alarm of smoke detector D. These results are nearly the opposite of those for detector A, which was more responsive to less intense fires than the CO detector. Detector D is more responsive to fires with higher smoke concentrations than the CO-1 detector.

At Stations 1 and 6, a smoke detector of type E was positioned near the roof adjacent to a CO-1 CO detector. For each experiment, an alarm was defined for detector E as the average background signal less 10 standard deviations of the detector's noise under ambient conditions. For normal airflow experiments 3-9, smoke detector E alarmed an average of 49 s before the CO-1 detector at Station 1, and 73 s earlier at Station 6. The longer average lag time at Station 6 compared to Station 1 is a result of the dilution of the CO as it traverses from Station 1 to Station 6. For reduced airflow experiments 10-12, the lag time was longer than for normal airflow conditions. At Station 1, the average lag time was 110 s, and at Station 6, the average lag time was 262 s for experiments 10-12. For experiment 11, smoke detector E alarmed at Station 6 while the CO concentration did not reach its alarm value. Figure 7 shows a comparison of the responses of smoke detector E and the type CO-1 CO detector at Station 6 for experiment 4. Smoke detector E and CO detector CO-1 have nearly simultaneous initial responses. The time lag observed in the peak response of the CO detector with respect to smoke detector E in figure 7, is due to the finite chemical reaction rate of the CO detector's chemical cell. This was also the case for a CO detector's response compared to smoke detector D's response.

Two factors that can affect fire detection in a mine are the growth in the smoke-particle diameter d and decrease in the smoke particulate number concentration, n, as the smoke traverses the mine entries. This effect has been described as a rate process (*8*). The proposed model equation is

$$\frac{1}{n} = kt + \frac{1}{n_o}, \qquad (1)$$

where t is the elapsed time the particles are in suspension, n_o is the initial smoke particulate concentration, and the coagulation coefficient, k, is approximated as 0.6×10^{-15} m^3/(particle · s) (*8*). The number concentration is related to the mass concentration, C_m, by

$$C_m = \frac{\pi}{6} d^3 \rho n, \qquad (2)$$

where ρ is the smoke mass density. C_m can be determined from a measurement of the optical transmission, T, over a path length, ℓ, using the Bouguer-Lambert law (*9*), which can be rewritten as

$$C_m = -\frac{2\rho d}{3Q\ell} \ln\left(\frac{T}{100}\right), \qquad (3)$$

where Q is the extinction coefficient. Equations 2 and 3 yield

$$n = -\frac{4}{\pi} \frac{\ln\left(\frac{T}{100}\right)}{Q\ell d^2}. \qquad (4)$$

Equations 1 and 4 can be used to evaluate the reduction in particulate number concentration. For example, for experiment 4, the minimum measured optical transmission at the light obscuration meter was 60 pct, which occurred 450 s after ignition of the fuel. With an approximate extinction coefficient, Q = 2, and an assumed smoke particle diameter of 0.5 μm when

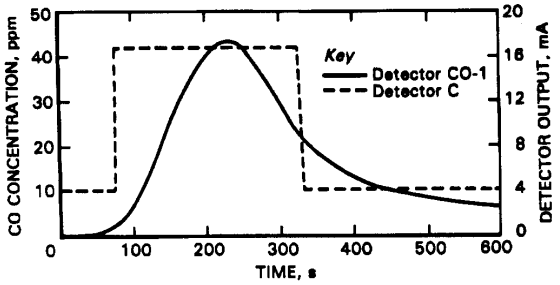

Figure 5.—Comparison of measured CO concentration and response of smoke detector C at Station 4 for experiment 4.

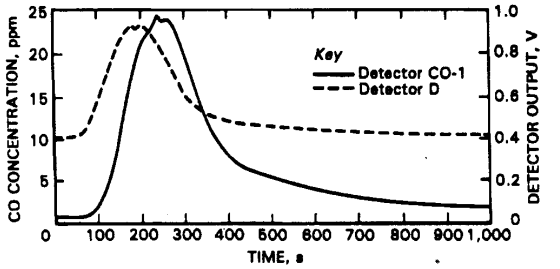

Figure 6.—Comparison of measured CO concentration and response of smoke detector D at Station 5 for experiment 4.

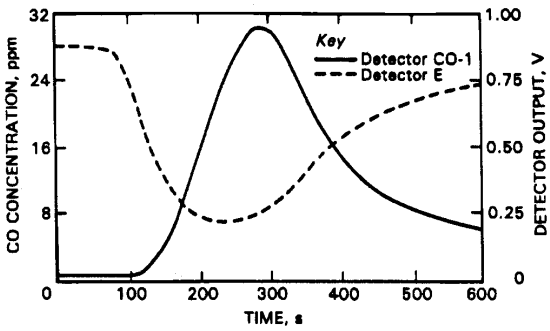

Figure 7.—Comparison of measured CO concentration and response of smoke detector E at Station 6 for experiement 4.

the smoke reaches the light obscuration meter, the calculated reduction in the expected number concentration of smoke particles is 35 pct as the smoke traverses the distance from the fire to the light obscuration meter, when the optical transmission is 60 pct. A reduction in particle number concentration is associated with an increased particle diameter based upon the assumption of constant mass concentration. The implication of this calculation is that for a 35 pct reduction in particle concentration to that associated with a particle diameter of 0.5 μm, the smoke particle diameter at the fire would be 0.43 μm. This represents a 16 pct increase in smoke particle diameter.

Additional measurements are required with regard to smoke particulate diameter, such as with a three-wavelength optical detector as described in previous work (*10*), before a more definite conclusion can be drawn regarding particulate coagulation.

Equation 3 implies that, for a smoke cloud with a constant mass concentration, the quantity, d ln (T)/Q, is constant. The ratio of Q to d is constant over a small range of particulate diameter. This is based upon calculated values of Q which show a monotonic decrease with respect to decreases in d. Since over a small range of diameters the quantity d/Q is nearly constant, the implication is that the optical transmission, T, is nearly constant. This implies that coagulation could affect an ionization-type more than an optical-type smoke detector.

Measurement of the arrival time of specific CO concentrations at the beginning (Station 1) and end of F Butt (Station 6) provides information on the effect of crosscuts on CO transport time. Table 4 shows the measured travel time of the CO concentration, which is 5 ppm above background from Station 1 to Station 6 for experiments 3-12. A CO concentration 5 ppm above background is considered to be the alarm value for this study. Experiments 1 and 2 were excluded because the CO concentration was too low. For experiments 10 and 12, the 5 ppm CO concentration above background was nearly at the maximum measured CO concentration in those tests. For experiment 11, the maximum CO concentration at Station 6 was less than 5 ppm. Figure 8 shows typical CO concentration profiles at Station 1 and Station 6, which are 91 m apart, as measured with a diffusion-mode CO-1 detector for experiment 4. The flat portion in the concentration profile at Station 1 between 150 and 200 s is because the maximum detector range of 50 ppm was exceeded. The reduction in the maximum CO concentration at Station 6 is caused by the entrainment of CO at crosscuts.

Table 4.—Measured CO alarm and smoke response travel times and predicted travel times, seconds

Experiment	Measured			Predicted	
	CO	Smoke[1]	Smoke[2]	τ_e	τ_{ec}
3.....	111	100	96	101	101
4.....	122	104	101	96	153
5.....	110	94	94	100	100
6.....	122	96	85	97	124
7.....	127	110	100	98	127
8.....	136	104	107	106	166
9.....	130	102	108	99	99
10	548	532	1,390	267	448
11	NA	1,110	428	299	472
12	777	1,032	618	355	561

NA Not available.

[1]Based upon maximum signal from smoke detector E.

[2]Based upon detector E's average background signal less ten standard deviations of detector's noise under ambient conditions.

An analysis was made of the CO travel times between alarms at seventeen pairs of CO-1 sensors in F Butt. This included the path from Station 1 to Station 6, a 91-m separation, for experiments 3-8; the path from Station 3 to Station 6, a 71-m separation, for experiments 3-8; and the path from Station 3 to Station 4, a 26-m separation, for experiments 3-8, exclusive of experiment 4, which yielded an outlier. A correlation of the measured travel time, τ_m, between alarms at the ends of the path with τ_e and τ_{ec} yielded

$$\tau_m = \tau_e(\tau_{ec}/\tau_e)^{0.67}, \quad (5)$$

where τ_e is the predicted travel time based upon measured entry airflow and entry volume, and τ_{ec} is the predicted transport time based upon measured entry airflow and total volume, entry and crosscuts. Figure 9 shows a plot of τ_m/τ_e with respect to τ_{ec}/τ_e, as well as the correlation equation (equation 5). The standard deviation of the regression was 0.1. The exponent 0.67 in equation 1 is in close agreement with the exponent 0.62 determined from the analysis of CO release experiments and reported by Friel and others (*4*) as equation 2. The data for experiment 9 were treated as an outlier. This is consistent with the experimental observation that the detector cell for the CO detector at Station 6 had deteriorated for experiment 9. The analysis developed in (*4*) applies to the measured transport time of CO concentration less than the half-height of the maximum CO concentration. Experiments 10-12 were for reduced airflow and resulted in CO concentration at Station 6 for which half the maximum CO concentration was less than 5 ppm above background and, therefore, these experiments were excluded from the correlation.

The significance of using CO detectors with the same operating characteristics to evaluate the transport time of a specific CO concentration between stations, is demonstrated through a comparison of the responses of types CO-1 and CO-2 detectors, which have different operating characteristics, at the same station. A comparison was made at Station 6 of the CO levels measured by the CO-1 and CO-2 detectors. Figure 10 shows the measurable responses for experiment 4 of each CO detector. The measured values for CO-2 were mathematically smoothed. There are three major observations with regard to figure 10. First, the diffusion-mode CO detector, CO-1, responds earlier than the pump-mode detector, CO-2. Second, the maximum CO concentration is lower for the diffusion-mode detector. Third, based upon a 5-ppm alarm setting, both detectors yield an alarm at the same time. These observations were repeatable for experiments 5, 6, and 7, for which measurements of CO responses with CO-1 and CO-2 detectors were both available. The CO detectors differed not only in the diffusion versus pump mode, but in the chemical cell used to detect the CO. Both factors account for the different responses of the detectors. Based upon the faster delivery rate of CO to the detector with a pump than through diffusion, it is expected that the real-time CO concentration is more closely represented by the results from CO-2. Because differences in arrival times are considered in the crosscut analysis presented above, it is necessary to use CO detectors of the same measurement and response characteristics for that analysis.

A simple mathematical model can be constructed to explain the response of the diffusion-mode detector. Let the true CO concentration be denoted by C_e, and the measured CO concentrations by C. The measured CO concentration in the diffusion-mode detector lags C_e due to diffusion in the entry tube of the detector, diffusion through the membrane covering the

detector's chemical cell, and chemical reaction in the cell. These three processes can be described by an effective rate constant, k, which is the reciprocal of an effective time constant associated with these processes. The assumption of a first-order linear rate process results in the model equation,

$$\frac{dC}{dt} = -k(C-C_e). \qquad (6)$$

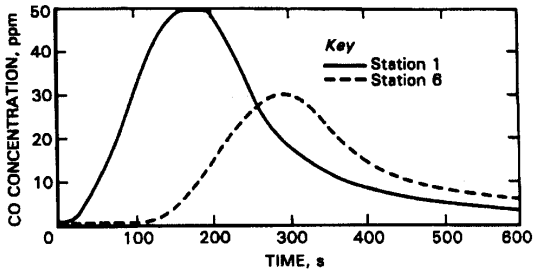

Figure 8.—Comparison of CO concentration at the beginning and end of F Butt for experiment 4.

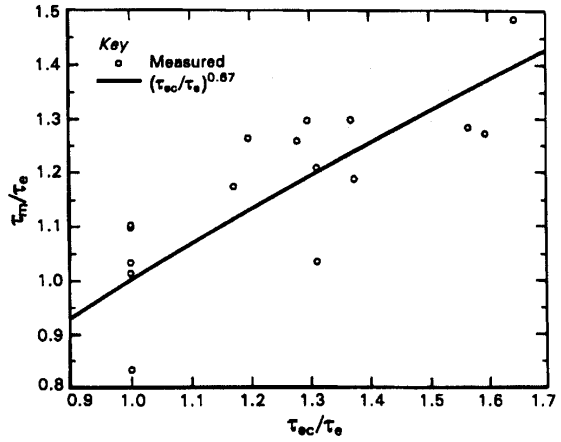

Figure 9.—Correlation of τ_m/τ_e with τ_{ec}/τ_e for CO detector separations of 26, 71, and 91 m.

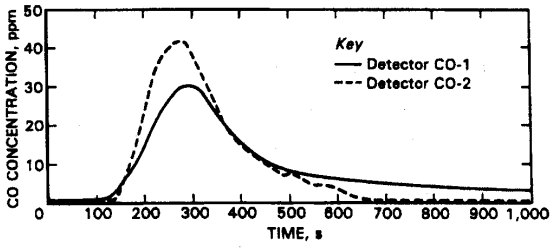

Figure 10.—Comparison of response of CO detectors CO-1 and CO-2 at Station 6 for experiment 4. Data for detector CO-2 have been smoothed.

Equation 6 was applied to an assumed triangular distribution of CO, C_e, shown in figure 11 as an approximation to the values measured with detector CO-2. The functional form of the driving term, C_e, was

$$\begin{aligned} C_e &= C_1 t/t_1, \quad 0<t<t_1 \\ &= C_1(1-(-t-t_1)/t_1), \quad t_1<t<2t_1 \\ &= 0 \qquad\qquad t>2t_1. \end{aligned} \qquad (7)$$

Based upon the observed value from detector CO-2 in figure 10, the model application was made with C_1 = 45 ppm and t_1 = 146 s. The time axis was shifted so that the rise in the CO concentration coincides with the first measurable response of the CO-1 detector. An analytic solution was developed as a solution to the model, equation 6, and the driving term C_e, in equation 7. A time constant equal to 90 s was used to define the rate constant, k = 1/90 s^{-1}. The model equation solution, C, is shown in figure 11 along with the driving term, C_e, and the measurement from detector CO-1. The model yields very good agreement with the measured CO from the initial detection to the inflection point of the curve on the decreasing side of the CO concentration curve. Discrepancy beyond the inflection point is possibly due to the assumed symmetrical distribution of the actual CO concentration, C_e. In reality, the processes of convection and dispersion along the airway and CO entering and leaving crosscuts are expected to produce an asymmetrical distribution of CO. The model shows the linear rate assumption is realistic.

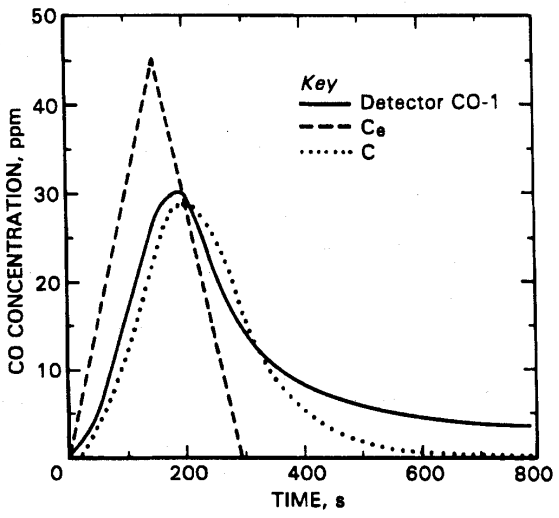

Figure 11.—Comparison of model prediction of CO concentration at Station 6 with CO measurement for experiment 4.

Figure 12 shows the responses of two smoke detectors of type E located at Stations 1 and 6 for experiment 4. The two curves are similar in shape. There is not the significant attenuation in the detector's maximum response at Station 6 as was shown for the CO response at Station 6 in figure 8. The data in table 4 show that the measured time difference between peak values of detector E's response to smoke is approximately equal to τ_e, regardless of whether the crosscuts are accessible for experiments 3-9. This could be possibly caused by the micron size dimension of the smoke particulates compared to the molecular dimension of the CO. This size difference could result in less entrainment of smoke than of CO into the crosscuts. This is a conjecture that requires verification. For reduced airflow experiments 10-12, smoke detector E's measured smoke travel times based upon peak signal were significantly greater than τ_{ec}, as shown in table 4. These reduced-flow cases resulted in significant attenuation of the peak signal of detector E at Station 6 compared to Station 1, unlike experiments 3-9, which had comparable peak signal responses at both stations. Table 4 further shows that for normal airflow experiments 3-9, a measurement of smoke travel time based upon an alarm signal for smoke detector E as defined earlier, is not appreciably different than travel time based upon the maximum signal.

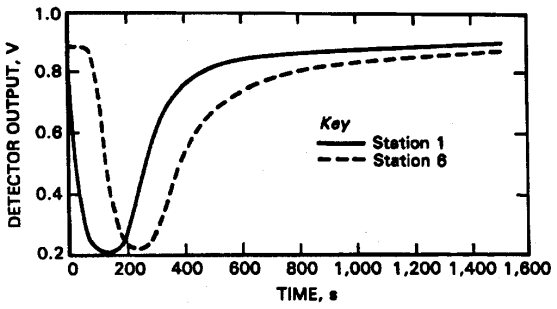

12.—Comparison of response of smoke detector E to smoke at the beginning and end of F Butt for experiment 4.

CONCLUSIONS

From the results of this study, several conclusions can be drawn.

1. Pump-mode, optical-type smoke detector A demonstrated increased signal response for less intense diesel-fuel fires as characterized by smoke intensity, when compared with the CO alarm of a diffusion-mode CO detector, CO-1. For the less intense fires, smoke detector A alarmed prior to CO-1, and for the more intense fires the opposite alarm sequence occurred.

2. A comparison of pump-mode ionization-type smoke detector B, and a diffusion-mode CO detector, CO-1, for diesel fuel fires, showed that the smoke detector consistently alarmed before the CO detector. The CO alarm occurred at an average optical density of 0.085 m^{-1}, whereas the smoke detector alarm occurred at an average optical density of 0.021 m^{-1}.

3. The diffusion-mode, ionization-type smoke detector, detector C, alarmed for those experiments for which the optical density was greater than 0.15 m^{-1}. Its alarm occurred prior to the alarm of the CO-1 CO detector.

4. The diffusion mode, optical-type smoke detector, detector D, alarmed in all cases earlier than the CO detector, CO-1. It also alarmed in two experiments for which the CO concentration was less than its alarm value.

5. The diffusion-mode, ionization-type smoke detector, detector E, alarmed for each experiment earlier than the CO detector, CO-1, and alarmed for one experiment for which the CO concentration was less than its alarm value.

6. A correlation made of the transport time of 5 ppm above background CO between three pairs of detectors separated by 26, 71, and 91 m for six diesel fuel fire experiments, showed that the travel time can be estimated by $\tau_e (\tau_{ec} / \tau)^{0.67}$. The exponent, 0.67, is only slightly greater than the exponent of 0.62 determined from CO release experiments (*4*).

7. The transport time of smoke over 91 m, as measured by smoke detector E, did not show a dependence on crosscut volume under normal airflow conditions.

8. From an evaluation of the burning rate of diesel fuel for mine diesel fuel fire experiments with convective airspeed of 2 m/s and one experiment with lower airspeed, about 0.4 m/s, the fuel burning rates were lower than the values of the rate reported elsewhere (*5*) for zero airflow conditions.

9. Visual observation of flame tilt indicated a tilt of 47° to 59° from the normal to the fuel surface, whereas previous experimental correlations (*6-7*) predicted 76° and 70°.

10. An estimation of the coagulation of smoke particles demonstrated that this effect could reduce the smoke particulates number concentration by 35 pct and correspondingly increase the smoke particulate's average diameter by 16 pct, for a 450-s smoke travel time. This could affect the response characteristic of a smoke detector.

Based upon this set of diesel-fuel fire experiments, it is recommended that smoke detectors that have a continuous analog output signal be used whenever possible as part of a mine atmospheric monitoring system. These sensors would give greater flexibility for setting alarm values for fire detection at low smoke levels. Smoke detectors that require relatively low maintenance, such as diffusion-mode detectors, have a reasonable expectation of being at least as effective as CO detectors. Based upon results from experiments with one pair of ionization-type, diffusion-mode smoke detectors, the effect of crosscuts on smoke travel time would be minimal for a particular smoke

detector alarm level under normal airflow conditions. This aspect would be incorporated in a mine fire location strategy. Smoke detectors, when incorporated into a mine atmospheric monitoring system, will complement CO detectors and thereby improve mine safety.

ACKNOWLEDGMENT

The authors wish to acknowledge Gerald S. Morrow, Electronics Technician, USBM Pittsburgh Research Center, for providing technical assistance in preparation for the mine fire experiments.

REFERENCES

1. Morrow, G. S., and C. D. Litton. In-Mine Evaluation of Smoke Detectors. USBM IC 9311, 1992, 13 pp.

2. Edwards, J. C., and G. S. Morrow. Development of Coal Combustion Sensitivity Tests for Smoke Detectors. USBM RI 9551, 1995, 12 pp.

3. __. Evaluation of Smoke Detectors for Mining Use. USBM RI 9586, 1995, 17 pp.

4. Friel, G. F., J. C. Edwards, and G. S. Morrow. Effect of Dead-End Crosscuts on Contaminant Travel Times in Mine Entries. USBM RI 9517, 1994, 18 pp.

5. Burgess, D. S., J. Grumer, and H. G. Wolfhard. Burning Rates of Liquid Fuels in Large and Small Open Trays. Ch. in The Use of Models in Fire Research. Nat. Acad. Sci.-Nat. Res. Council, Pub. 786, 1961, pp. 68-75.

6. Thomas, P. H. The Size of Flames from Natural Fires. Paper in Proceedings of the Ninth Symposium (International) on Combustion (Ithaca, NY, Aug. 27-Sept. 1, 1962). The Combustion Inst. (Academic Press, New York), 1963, pp. 844-859.

7. National Fire Protection Association. SFPE Handbook on Fire Protection Engineering. National Fire Protection Assn., Quincy, MA, 1988, pp. 2-52.

8. McPherson, M. J. Subsurface Ventilation and Environmental Engineering. Chapman & Hall, New York, 1993, pp. 778-781.

9. Hottel, H. C., and A. F. Sarofin. Radiative Transfer. McGraw-Hill Book Co., New York, 1967, p. 201.

10. Cashdollar, K. L., C. V. Lee, and J. M. Singer. Three-Wavelength Light Transmission Technique To Measure Smoke Particle Size and Concentration. Appl. Optics, v. 18, No. 11, June 1, 1979, pp. 1763-1769.